Simple algorithm for designing skew-quadrupole cooling configurations

2006 New J. Phys. 8 286

(http://iopscience.iop.org/1367-2630/8/11/286)

New Journal of Physics
The open-access journal for physics

Simple algorithm for designing skew-quadrupole cooling configurations

Bruce E Carlsten and Kip A Bishofberger
Los Alamos National Laboratory, Los Alamos, NM 87545, USA
E-mail: bcarlsten@lanl.gov

New Journal of Physics **8** (2006) 286
Received 18 May 2006
Published 28 November 2006
Online at http://www.njp.org/
doi:10.1088/1367-2630/8/11/286

Abstract. Previous discussions of skew-quadrupole channels for emittance cooling have lacked a clear prescription of how to design a specific configuration. We present simple formulae that can be used to design such a channel for a beam entering at a waist. A nominal design is presented for a 120 kV, 2 A electron beam that requires 433 G of axial field at the cathode and three skew-quadrupoles with reasonable field gradients in a 10 cm long region. This design leads to a final emittance ratio of nearly three hundred.

Contents

PII: S1367-2630(06)24858-4

1. Introduction

It has been shown theoretically [1]–[3] and partially verified experimentally [4] that three skew-quadrupoles can transform a round electron beam with angular momentum into a sheet beam with a large aspect ratio and a large emittance ratio, while preserving the product of the transverse emittances. This conversion process is of interest for future linear–collider applications, where asymmetric beams can lead to higher luminosities, and for low-energy, high-frequency microwave sources that use sheet electron beams.

Sheet beams intended for miniaturized high-power rf sources at 100 GHz and higher frequencies are typically emittance-dominated in the thin dimension and space–charge-dominated in the wide dimension. Beam emmittances from thermal and nonlinear focusing effects in conventional electron gun technology have been adequate for previous experiments done at 100 GHz [5]–[7], but are approaching the stability limit for both periodic permanent-magnet and wiggler-focusing configurations [8, 9]. These beam emittances are not adequate for higher frequencies such as 200–300 GHz. Lowering the beam current or cooling the beam emittance (in the thin plane) is necessary for useful production of rf at these higher frequencies. The emittance-transfer mechanism studied in [1]–[4] is very attractive for this type of high-power, high-frequency source. Because the wide dimension is space–charge limited, it can absorb a significant increase in emittance without degradation to its transport.

The cooling scheme begins by immersing the cathode in a solenoid field, which provides canonical angular momentum to the beam. When the beam exits the solenoid, the beam begins to rotate, which leads to an effective emittance growth. Three skew quadrupoles are then used to eliminate this growth (so the product of the final horizontal and vertical emittances is the same as the product of the beam's intrinsic emittances), while making one emittance much smaller than the other. Skew quadrupoles are rotated at a 45° angle from the nominal vertical and horizontal axes and have forces as shown in figure 1.

The horizontal force on a particle is proportional only to its vertical displacement, and the vertical force is proportional to its horizontal displacement. Let us consider the case of minimizing the beam's horizontal emittance. The strength of the first skew-quadrupole is set to nearly stop the horizontal rotation, but it adds to the vertical rotation, making the beam form a diagonal shape as it drifts to the second skew-quadrupole. Because the beam shape is no longer round at this position, the second quadrupole changes the beam's angular momentum, forcing the diagonally oriented beam to rotate towards the vertical axis. The final skew-quadrupole is located where the diagonal beam rotation reached the vertical axis, and its strength is set to stop the particles' horizontal motion (eliminating the angular momentum), leaving only vertical motion roughly proportional to vertical position. This process will be shown later in detail in section 3.

Using unique properties of symplectic transformations, Kim [3] derived the maximum ratio of the final emittances to be

$$\frac{\varepsilon_{\text{larger}}}{\varepsilon_{\text{smaller}}} \approx \left(\frac{2\mathbf{L}}{\varepsilon_{\text{intrinsic}}}\right)^2, \tag{1}$$

where $\varepsilon_{\text{intrinsic}}$ is the beam's intrinsic emittance (without angular momentum) and $\mathbf{L}$ is the quadrature emittance contribution of the canonical angular momentum,

$$L = \frac{eB_{\text{cath}}R_{\text{cath}}^2}{16\gamma\beta cm}, \tag{2}$$

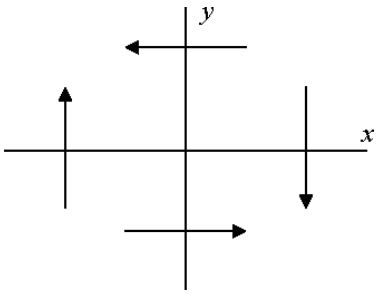

Figure 1. Force orientation of a skew-quadrupole.

under the limit $\mathbf{L} \gg \varepsilon_{\text{intrinsic}}$, where γ and β are the beam's relativistic mass factor and normalized relativistic velocity respectively, e is the electronic charge, m is the electronic mass, c is the speed of light, B_{cath} is the axial magnetic field at the cathode and R_{cath} is the radius of the beam's cathode. This maximum ratio is reached whenever the ensemble-averaged correlations $\langle xy' \rangle$ and $\langle x'y \rangle$ are made to vanish, independent of the specific design of the entire channel. Kim also derived three scalar equations that, when satisfied, remove these cross-correlations from a round beam that possesses angular momentum. He suggested using three quadrupole strengths as the three parameters to satisfy these conditions (with drift lengths acting as free parameters). We alternatively choose two quadrupole strengths and cathode axial field as our three parameters, as first explored by Burov *et al* [10]. Additionally, the phase advances of the two transverse motions must differ by 90° [1, 2] for the case of an arbitrary initial beam.

The required transfer matrix for the emittance conversion scheme does not depend on the intrinsic beam emittance, so the zero-emittance case can be analysed and applied to the general situation. This fact greatly simplifies the analysis, since the beam size and divergence of the beam vanishes when the intrinsic emittance is zero. The next section shows that, for a beam initially at a waist, setting the final horizontal size and divergence to zero dictates values for three free parameters. A beam with nonzero intrinsic emittance, evolved through the same cooling channel, will possess a product of its horizontal and vertical emittances equal to the product of the original intrinsic emittances, as desired. It should be pointed out that space–charge forces deform a beam lacking cylindrical symmetry, so the correlations $\langle xy' \rangle$ and $\langle x'y \rangle$ are no longer forced to vanish for a beam with nonzero current. However, this effect is small for the case considered.

The cooling procedure is straight forward to describe qualitatively, but a simple procedure for specifying the quadrupole attributes (location and strength) has eluded previous analyses. The following section presents such formulae to generate a channel under some convenient assumptions. In particular, we take the case where the quadrupoles are equally spaced and the focal length of the centre one is twice the distance between the quadrupoles. We use the thin-lens approximation for the quadrupoles in order to find simple expressions for the quadrupole focusing strengths. These formulae are then used to design a channel for a 120 keV, 2 A electron beam suitable for a 300 GHz travelling wave tube amplifier. Finally, we show results of a particle-pushing code whose calculated emittance ratio for this channel very closely obeys equation (1). The simulation results also confirm that similar results are reached with quadrupoles of nonzero length.

2. Design formulae

We assume the beam is initially round and at a waist where it enters the first quadrupole. A general particle has initial coordinates (x_0, y_0) and initial divergence $(-Ay_0, Ax_0)$, where the constant A is related to the axial field on the cathode by

$$A = \frac{e}{2\gamma\beta mc} B_{\text{cath}} \left(\frac{R_{\text{cath}}}{R_{\text{beam}}} \right)^2, \tag{3}$$

where the last factor is the squared ratio of the beam size at the cathode to the beam size at the quadrupole. The initial divergence corresponds to a beam waist with nonzero angular momentum but without any intrinsic emittance. This waist condition is easily generated with a solenoid surrounding the cathode; the beam inside the solenoid possesses canonical angular momentum, and when the beam emerges from the solenoid, it begins to rotate.

Immediately after the third quadrupole, the horizontal position and divergence of the particle should be zero. While either of these conditions would satisfy the goal of zero horizontal emittance, both are necessary to ensure that the two correlations described in the previous section vanish. Surprisingly, these requirements lead to fairly simple design requirements. For this analysis, we assume the quadrupoles have zero length and we ignore space–charge forces.

We let the change in particle divergence through the first quadrupole be given by $(\Delta x', \Delta y')_{\text{Q1}} = (Cy_0, Cx_0)$, where C is related to the quadrupole field length integral by

$$C = \frac{e}{\gamma\beta mc} \int B'_{\text{Q1}} \, \mathrm{d}l, \tag{4}$$

where B'_{Q1} is the field gradient of the first quadrupole and the integral covers its axial length. After the first quadrupole, the beam position is still (x_0, y_0) and the beam divergence is given by $(\delta y_0, \alpha x_0)$, such that

$$A = \frac{\alpha - \delta}{2} \quad \text{and} \quad C = \frac{\alpha + \delta}{2}. \tag{5}$$

After a drift of length L to the second quadrupole, the particle's position is given by:

$$(x_2, y_2) = (x_0 + \delta L y_0, y_0 + \alpha L x_0). \tag{6}$$

The particle's divergence is still $(\delta y_0, Ax_0)$ before the quadrupole. The particle's divergence is altered by $(\Delta x', \Delta y')_{\text{Q2}} = (-\eta y_2, -\eta x_2)$ due to the second quadrupole, resulting in a divergence:

$$(x'_2, y'_2) = [\delta y_0 - \eta(y_0 + \alpha L x_0), \alpha x_0 - \eta(x_0 + \delta L y_0)], \tag{7}$$

where $\eta = \frac{e}{\gamma\beta mc} \int B'_{\text{Q2}} \, \mathrm{d}l$. A length M from the second quadrupole to the third leads to the position:

$$(x_3, y_3) = [x_0 + \delta L y_0 + M(\delta y_0 - \eta(y_0 + \alpha L x_0)), y_0 + \alpha L x_0 + M(\alpha x_0 - \eta(x_0 + \delta L y_0))]. \tag{8}$$

The horizontal divergence, being $\delta y_0 - \eta(y_0 + \alpha L x_0)$ before the third quadrupole and changed by $\Delta x' = \zeta y_3$, becomes

$$x'_3 = \delta y_0 - \eta(y_0 + \alpha L x_0) + \zeta[y_0 + \alpha L x_0 + M(\alpha x_0 - \eta(x_0 + \delta L y_0))], \tag{9}$$

where $\zeta = \frac{e}{\gamma\beta mc}\int B'_{\mathrm{Q3}}\,\mathrm{d}l$. Denoting the final particle horizontal position and divergence by:

$$\begin{aligned} x_{\mathrm{f}} &= x_0 + \delta L y_0 + M[\delta y_0 - \eta(y_0 + \alpha L x_0)] \\ x'_{\mathrm{f}} &= \delta y_0 - \eta(y_0 + \alpha L x_0) + \zeta[y_0 + \alpha L x_0 + M(a x_0 - \eta(x_0 + \delta L y_0))], \end{aligned} \tag{10}$$

we set both x_{f} and x'_{f} to zero, for all initial values of x_0 and y_0. Setting $x_{\mathrm{f}} = 0$ provides the constraints

$$1 = ML\alpha\eta \tag{11}$$

and

$$M\eta = \delta(L + M). \tag{12}$$

Setting $x'_{\mathrm{f}} = 0$ additionally sets

$$\eta = \zeta + \delta(1 - ML\zeta\eta). \tag{13}$$

The fourth constraint, requiring the coefficient of y_0 in the $x'_{\mathrm{f}} = 0$ equation to vanish, is automatically satisfied by the other three constraints and is consistent with previous analyses [1]–[3], [10], which observed that only three parameters are required to remove the beam's cross-correlations, in turn leading to zero horizontal beam size and divergence when the intrinsic beam emittance is neglected.

For convenience, we set the drift lengths L and M equal, and the constraints become:

$$1 = L^2\alpha\eta, \qquad \delta = \eta/2, \qquad \zeta = \frac{\eta}{2 - L^2\eta^2}. \tag{14}$$

These three equations fully define the quadrupole channel, and lead to an infinite number of possible solutions. In general, the quadrupoles should not overfocus the beam; specifically, the focal length of the quadrupoles ought to be greater than their separation, so letting $L\eta = 1/2$ further refines our constraints. The other parameters are now fixed, and the complete solution for the quadrupole strengths and axial field on the cathode is:

$$\eta = 1/(2L), \qquad \delta = \eta/2, \qquad \alpha = 4\eta, \qquad \zeta = 4\eta/7, \tag{15}$$

where the actual quadrupole strengths and the axial field on the cathode are found using equations (3)–(5).

Previous analyses solved for a transfer matrix from just before the termination of the solenoid to the final quadrupole. The 2×2 transfer matrices of the two transverse dimensions differ by a 90° phase shift [1, 10]. The total transfer matrix is of the form

$$T = \begin{pmatrix} 0 & \chi(c-s)/2 & 0 & \chi(c+s)/2 \\ 0 & -(c+s)/2 & 0 & (c-s)/2 \\ c-s & \chi(c+s)/2 & -(c+s) & \chi(c-s)/2 \\ -(c+s)/\chi & (c-s)/2 & (s-c)/\chi & -(c+s)/2 \end{pmatrix}, \tag{16}$$

where $c = \cos\mu$, $s = \sin\mu$, $\chi = 1/A$ from equation (3), and μ is the single free parameter. Explicit calculation of the transfer matrix of the solution presented here is surprisingly not of this form. This is due to our initial beam structure—we start with a beam at a waist, which provides an alternative degree of freedom in the overall channel design (which allows us to find solutions that do not require the 90° phase shift). This leads to having both M/L and the product $L\eta$ as free parameters. Because of this freedom, these solutions encompass the more constrained solution described by equation (16), plus other specific cooling designs. The additional requirement of having a beam waist at the location of the first quadrupole can be met with a single solenoid, so the solutions in equations (11)–(13) can also be considered as a subset of the class of solutions with four degrees of freedom.

3. Specific solution for a 120 keV electron beam

Using equations (15) with 5 cm drifts between the quadrupoles, we find:

$$\begin{aligned} &\eta = 10\,\mathrm{m}^{-1}, \qquad \delta = 5\,\mathrm{m}^{-1}, \qquad \alpha = 40\,\mathrm{m}^{-1}, \qquad \gamma = 5.714\,\mathrm{m}^{-1}, \\ &A = 17.5\,\mathrm{m}^{-1}, \qquad C = 22.5\,\mathrm{m}^{-1}, \end{aligned} \tag{17}$$

for a 120 keV beam, which lead to a field of 433 G on the cathode and field integrals of 278 G for the first quadrupole, 124 G for the second quadrupole, and 70.7 G for the third quadrupole.

We use the particle-pushing code PUSHER [8] to simulate the effect of this channel, starting with a beam that has a 5 mm radius. The quadrupoles in this simulation are assumed to be 0.4 mm long with a cosine-like axial field pattern. The initial simulation is for a beam with zero current and initial emittance in order to match the analysis.

For this numerical calculation, we use the normalized rms emittance given by:

$$\varepsilon_{x,\mathrm{norm}} = \beta\gamma\sqrt{\langle x^2\rangle\langle x'^2\rangle - \langle xx'\rangle^2}. \tag{18}$$

We use this approach to design an emittance-cooling channel for a 120 keV, 2 A beam with an intrinsic emittance of 6 mm mrad. This beam is adequate for a 100 GHz travelling wave tube amplifier [5, 6], but the emittance is about a factor of three too large for a 300 GHz amplifier. Our goal is to simulate a cooling channel leading to a final horizontal emittance less than 1 mm mrad. For the channel parameters above, the emittance contribution from the axial magnetic field at the cathode is about $\mathbf{L} = 76$ mm mrad. According to equation (1), the final emittance ratio will be about 640 and the final horizontal emittance approximately 0.25 mm mrad. This value is significantly better than the necessary emittance for a 300 GHz amplifier.

The results from PUSHER simulations agree well with the theory, predicting a final emittance ratio of about 660 and a final horizontal emittance of about 0.23 mm mrad. The simulated geometry is shown in figure 2. An iron pole piece at the end of the solenoid clamps the axial magnetic field and the solenoid length is adjusted to ensure a waist that the location of the first skew-quadrupole, while providing the right amount of axial field at the cathode. Figure 3 shows the beam shape and velocities just before and after the first quadrupole, and figures 4 and 5 show the same for the second and third quadrupoles. These results were obtained for the parameters given in equation (15), and they show remarkable agreement with the theoretical premise of a vanishing final horizontal emittance.

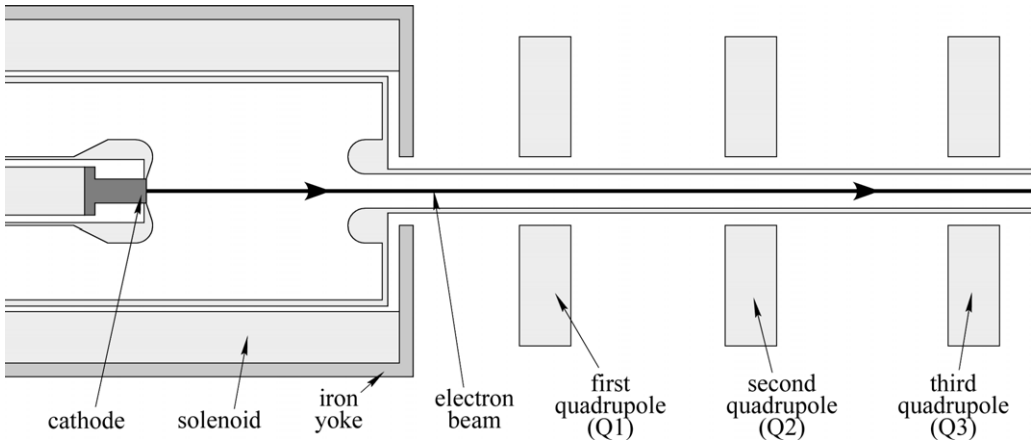

Figure 2. Schematic of an electron gun immersed in an axial magnetic field followed by three skew-quadrupoles. The beam profiles just before and after the first quadrupole are shown in figure 3, the second quadrupole in figure 4, and the third quadrupole in figure 5.

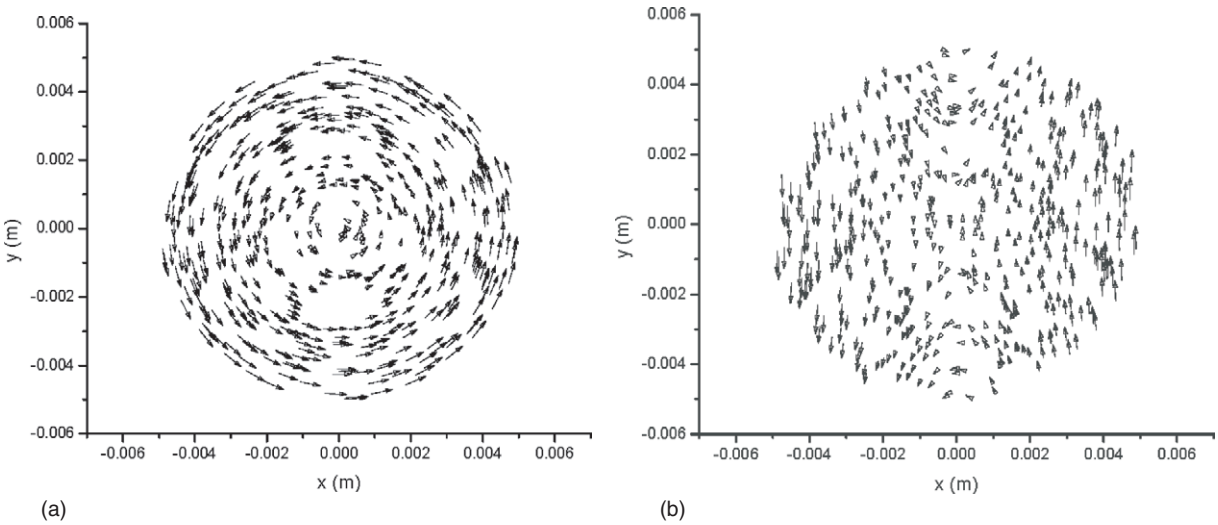

Figure 3. Beam shape and particle velocities just before (a) and just after (b) the first quadrupole.

Figure 3 confirms that the first quadrupole removes most of the horizontal motion. However, the small amount remaining is crucial to forcing $x_f = 0$.

Figure 4 shows that the second quadrupole actually increases the beam's angular momentum, and it sets the proper beam condition at the upcoming beam waist at the location of the final quadrupole.

Inspection of figure 5 shows that the beam's angular momentum has decreased to nearly zero, since the third quadrupole can put torque on the vertically aligned beam to stop its horizontal motion. A small amount of horizontal velocity remains (enlarged by the expanded horizontal scale), which leads to a spreading at the extreme ends of the distribution. Due to the finite size of

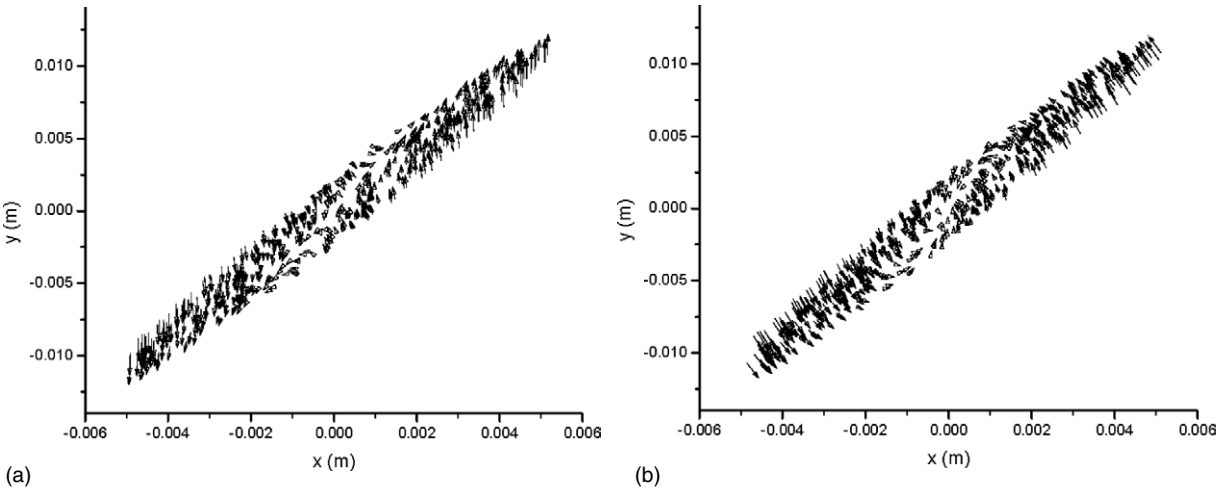

Figure 4. Beam shape and particle velocities just before (a) and just after (b) the second quadrupole.

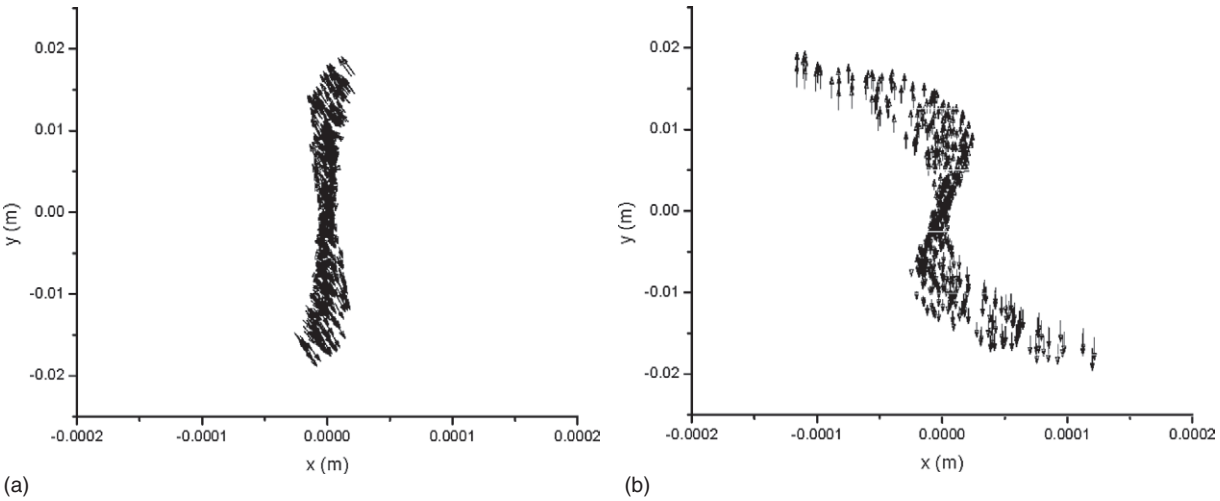

Figure 5. Beam shape and particle velocities just before (a) and just after (b) the third quadrupole. The horizontal axis is significantly enhanced from the previous figures.

the quadrupoles, the axial locations of the beam distribution that are plotted in figure 5 are slightly shifted to best show the evolution of the distribution. Figure 5(a) is 1.2 mm before the centre of the third quadrupole with the quadrupole turned off, and figure 5(b) is 0.8 mm after the centre of the third quadrupole (0.6 mm after its physical end). The small correlation that still exists after the third quadrupole (most likely due to nonlinearities in the transport from longitudinal and transverse coupling in the motion, possibly resolution issues with the magnetic field or the finite quadrupole lengths) corresponds to a very small emittance and beam width. In an experiment, a minor adjustment to the third quadrupole strength can compensate for any residual angular momentum.

Table 1. Emittances and beam sizes for specific simulation cases.

Input parameters	Horizontal emittance (mm mrad)	Vertical emittance (mm mrad)	Horizontal beam size (m)	Vertical beam size (m)	Emittance ratio
0 A, 0 mm mrad	2.2×10^{-4}	152	0.32×10^{-4}	9.13×10^{-3}	–
2 A, 0 mm mrad	0.117	153	2.56×10^{-4}	9.27×10^{-3}	–
0 A, 6 mm mrad	0.233	153	3.54×10^{-4}	9.14×10^{-3}	657
2 A, 6 mm mrad	0.541	153	4.61×10^{-4}	11.53×10^{-3}	283
0 A, 60 mm mrad	22.6	175	35.2×10^{-4}	9.77×10^{-3}	7.74

Table 2. Variation due to beam current and emittance for 1 cm long quadrupoles.

Input parameters	Horizontal emittance (mm mrad)	Vertical emittance (mm mrad)	Horizontal beam size (m)	Vertical beam size (m)	Emittance ratio
0 A, 0 mm mrad	9.7×10^{-4}	152	0.25×10^{-4}	9.52×10^{-3}	–
0 A, 6 mm mrad	0.267	153	3.67×10^{-4}	9.53×10^{-3}	573
2 A, 6 mm mrad	0.772	153	4.62×10^{-4}	9.69×10^{-3}	198

Using the channel optics described in the previous discussion, we summarize our simulation results using nonzero beam current and emittances in table 1. The first case, without space–charge or emittance, is an unrealistic simulation that nearly gives the infinite ratio predicted by equation (1). A 2 A beam with space charge shows a significant increase in the final horizontal emittance, though this is not included in the theoretical analysis.

The next two cases include 6 mm mrad of intrinsic emittance with and without space charge. Comparing the two, the horizontal emittance degrades by about a factor of two, but it is still outstanding for future high-frequency amplifier applications. The final example employs a large intrinsic emittance, 60 mm mrad, but its results again approach the theoretical estimate even though the intrinsic emittance is nearly 80% of the emittance contribution from the beam's canonical angular momentum.

A more realistic quadrupole length of 1 cm was used for the results presented in table 2. Due to this, a small degradation in cooling performance can be observed. However, the resulting emittances and ratios are still quite impressive, and we believe that experimentally modifying the quadrupole strengths will recover some of the degraded performance.

References

[1] Brinkman R, Derbenev Ya and Floettmann K 2001 *Phys. Rev. ST Accel. Beams* **4** 053501
[2] Burov A, Nagaitsev S, Shemyakin A and Derbenev Ya 2000 *Phys. Rev. ST Accel. Beams* **3** 094002
[3] Kim K J 2003 *Phys. Rev. ST Accel. Beams* **6** 104002
[4] Edwards D *et al* 2001 *Proc. 2001 Particle Accelerator Conf.* (Piscataway, NJ IEEE) pp 73–75

[5] Carlsten B E, Russell S J, Earley L M, Krawczyk F L, Potter J M, Ferguson P and Humphries S 2005 *IEEE Trans. Plasma Sci.* **33** 85
[6] Carlsten B E, Russell S J, Earley L M, Haynes W B, Krawczyk F L, Smirnova E, Wang Z F, Potter J M, Ferguson P and Humphries S 2005 MM-wave source development at Los Alamos *Proc. 7th Workshop on High Energy Density and High Power RF, AIP Conf. Proc.* **807** 326
[7] Scheitrum G 2005 Design and construction of a W-band sheet beam klystron *Stanford Linear Accelerator Center Publication* SLAC-PUB-11688
[8] Carlsten B E, Earley L M, Krawczyk F L, Russell S J, Potter J M, Ferguson P and Humphries S 2005 *Phys. Rev. ST Accel. Beams* **8** 062001
[9] Carlsten B E, Earley L M, Krawczyk F L, Russell S J, Potter J M, Ferguson P and Humphries S 2005 *Phys. Rev. ST Accel. Beams* **8** 062002
[10] Burov A, Nagaitsev S and Derbenev Ya 2002 *Phys. Rev.* E **66** 016503